Proceedings of Meetings on Acoustics

DECEMBER 03 2025

Measurement and analysis of electric guitar neck admittance for digital waveguide models

Takuto Yudasaka; Gary Scavone; Mark Rau; Kenta Ishizaka

Proc. Mtgs. Acoust. 58, 035024 (2025)
https://doi.org/10.1121/2.0002142

Volume 58 http://acousticalsociety.org/

International Symposium on Musical and Room Acoustics

24-28 May 2025

Loyola University
New Orleans, Louisiana

Musical Acoustics

Measurement and analysis of electric guitar neck admittance for digital waveguide models

Takuto Yudasaka
Department of Research & Development, Yamaha Corporation, Hamamatsu, Shizuoka, 4300912, JAPAN; takuto.yudasaka@music.yamaha.com

Gary Scavone and Mark Rau
McGill University, Montreal, QC, CANADA; gary.scavone@mcgill.ca; mrau@mit.edu

Kenta Ishizaka
Yamaha Corporation, Hamamatsu, Shizuoka, JAPAN; kenta.ishizaka@music.yamaha.com

This study investigates the implementation of neck admittance in digital waveguide (DWG) models for electric guitars. Admittance measurements reveal that the neck affects string vibration as much as, or even more than, the bridge, and this effect significantly changes depending on the fret. Finite element analysis confirms that these fret-dependent variations in admittance arise from vibrational mode shapes. Admittance on all frets were implemented into the DWG model to synthesize string vibrations. A comparison between the synthesized and measured vibrations revealed consistent trends in fret-dependent damping rates, validating the accuracy of the model. These findings underscore the importance of adjusting neck admittance based on fingering to improve the precision of DWG models.

Proceedings of Meetings on Acoustics, Vol. 58, 035024 (2025); https://doi.org/10.1121/2.0002142.

1. INTRODUCTION

Physical models are valuable for verifying differences due to design changes in the early stages of musical instrument development. Among the various methods available, the digital waveguide model (DWG) offers ease of implementation and high numerical efficiency.

In a DWG, the influence of the guitar body is typically modeled as a reflection function. An acoustic guitar has two string supports: a nut and frets at the neck and a bridge at the center of the body. Of these, the reflection function of the bridge, which vibrates more strongly, is considered to be more important and has been measured.[1]

On the other hand, solid-body guitars exhibit reduced body vibration. Therefore, the neck exhibits relatively greater vibration, and its effect on string vibration cannot be neglected. Previous studies have reported that the neck admittance of semi-hollow electric guitars changes depending on fret position.[2] Therefore, in order to reproduce the tone differences that depend on the shape of the body of the electric guitar, it may be necessary to account for the neck admittance, which changes depending on the left-hand fingering.

In this study, we investigated fret-dependent admittance variations from both an experimental and analytical perspective, and attempted to reproduce these effects using the DWG model.

2. ADMITTANCE MEASUREMENTS

A. OBJECTIVES

To investigate fret-dependent variations in admittance, measurements were taken using an impact hammer and laser Doppler vibrometer.

B. METHODS

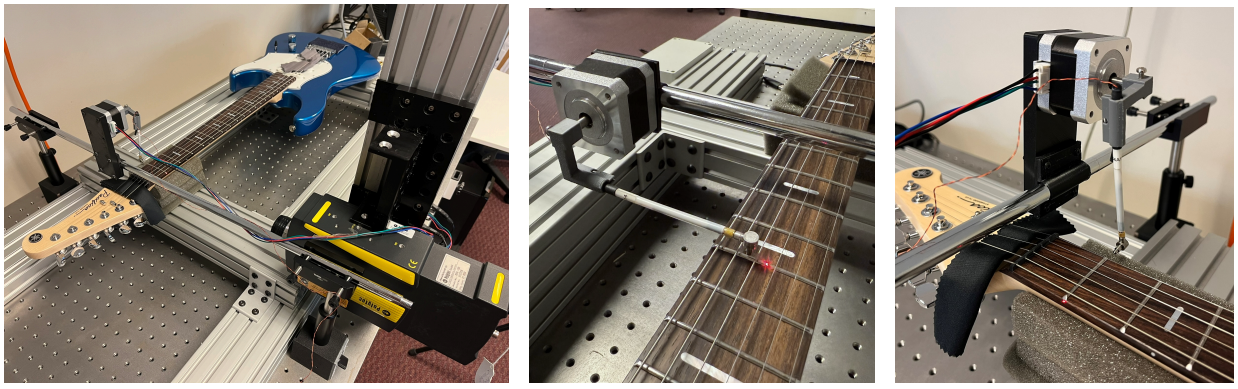

(a) Measurement system (b) Vertical measurement (c) Horizontal measurement

Figure 1: Admittance Measurement System

I. ELECTRIC GUITAR

A Yamaha Pacifica Standard Plus Series manufactured in 2024 was used for the measurements. This instrument has a solid body. Elixir 09-42 gauge strings were tuned to standard tuning and muted with cloths. The electric guitar was placed on a sliding structure on a vibration isolated table via soft foam (Fig. 1 (a)).

II. MEASUREMENT SYSTEM

A PCB PIEZOTRONICS Model 086E80 force-sensing impact hammer was used to excite the frets with a known impulse-like force. The hammer was set up to hit near the center of each fret (Fig. 1 (b)) and near the frets on the side of the neck (Fig. 1 (c)). To ensure consistent striking, an automated hammering device utilizing a stepper motor was used.[3]

A Polytec PDV-100 Laser Doppler Vibrometer was used to measure impulse-induced vibrations. The laser was aligned near the excitation point for vertical measurements and on the opposite side for horizontal measurements.

III. MEASUREMENT

A total of 24 vibration responses were measured—corresponding to the 22 frets, the nut, and the bridge. In the DWG model, string vibrations were represented as vertical and horizontal vibrations relative to the body, as well as the coupling of these.[4] Therefore, these admittances were measured using three configurations: vertical measurement as shown in Fig. 1(b), horizontal measurement as shown in Fig. 1(c), and a coupled measurement

with horizontal input and vertical output.[5] It is assumed that the vertical-input/horizontal-output configuration and its reciprocal yield equivalent results.[6]

IV. MEASUREMENT AND POST PROCESSING

Each location was measured five times, and outliers were excluded prior to averaging. Admittance, which characterizes the system's susceptibility to vibration, is defined in the frequency domain as follows:

$$\Gamma(\omega) \equiv \frac{V(\omega)}{F(\omega)},$$

where $V(\omega)$ is the velocity measured by the Laser Doppler Vibrometer, and $F(\omega)$ is the force measured by the impact hammer, both as functions of angular frequency ω.[7,8]

C. RESULTS

The results of the admittance measurements from each direction are shown in Fig. 2.

Figure 2(a) illustrates the vertical measurement results, showing prominent peaks around 175, 405, 640, and 900 Hz. Amplitude variations exceeding 40 dB are observed, depending on the fret position and frequency, because the different admittance peaks correspond to different mode shapes, each of which is position dependent along the neck. The mode shape for the peak at 175 Hz is illustrated in Fig. 5. While the amplitude of these resonances varies significantly, the corresponding frequencies remain nearly constant, reflecting the stability of the neck's natural vibrational modes.

Figure 2(b) presents the horizontal measurement results. The peaks are observed at different frequencies from Fig. 2 (a). This is because the vibration modes are different from those of vertical vibrations. Nonetheless, some modes—such as those at 175 Hz and 640 Hz—are common to both directions.

Figure 2(c) shows the results of the coupling configuration, where the amplitude is lower than in the vertical and horizontal cases, yet distinct peaks still appear. This suggests that vertical and horizontal string vibrations are coupled through the bridge, nut, and frets. The peak frequencies exhibit characteristics of both Fig. 2(a) and Fig. 2(b).

In all three figures, the thick line representing the bridge admittance is equal to or lower than the admittance at the frets and the nut. This implies that, in solid-body guitars, neck-side admittance (frets) is as influential as body-side admittance (bridge).

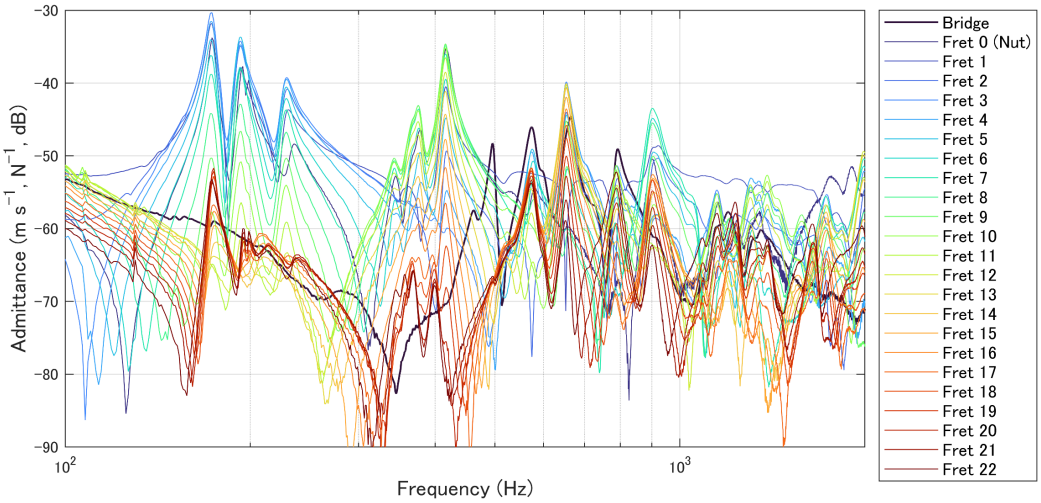

(a) Vertical measurement

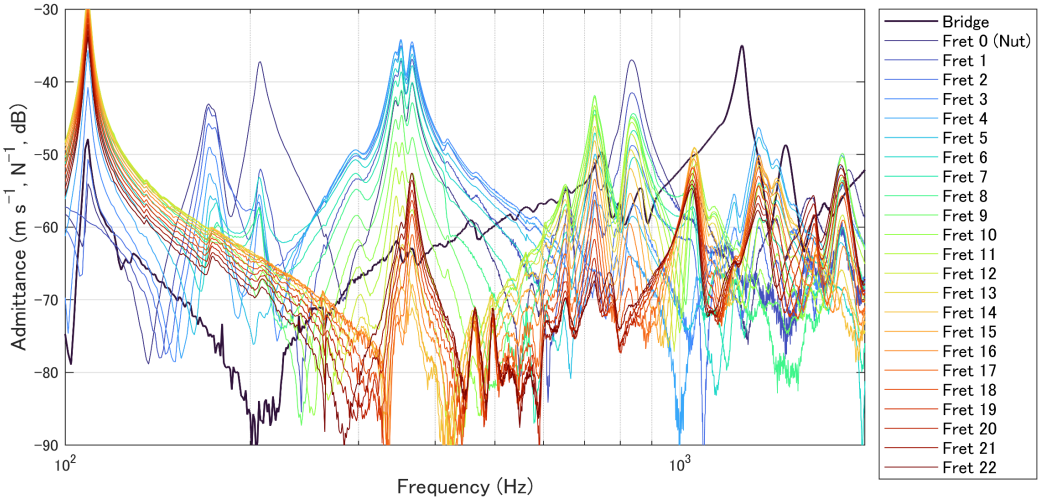

(b) Horizontal measurement

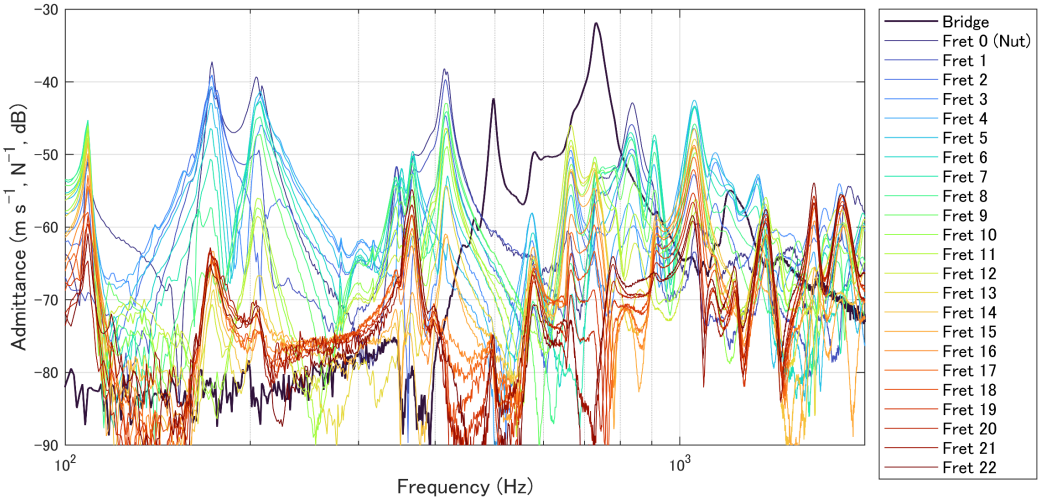

(c) Coupling measurement

Figure 2: Admittance measurement results from each direction

3. FINITE ELEMENT ANALYSIS

A. OBJECTIVES

To investigate the cause of the fret-dependent variations in admittance observed in the measurement results (Fig. 2), a finite element analysis (FEA) was conducted using a three-dimensional model.

B. METHODS

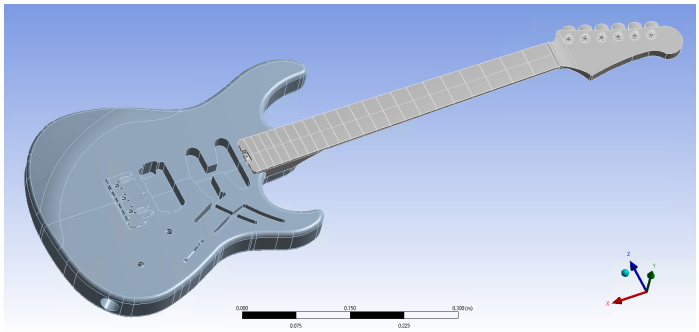

Figure 3: Finite Element Analysis Model of an Electric Guitar (Pacifica Standard Plus)

The three-dimensional CAD model of the measured guitar, imported into ANSYS, is shown in Fig. 3. This model accurately replicates the instrument's physical dimensions. The material properties of each component were appropriately assigned. As in the experimental setup, the lower sections of the neck and body were modeled as two elastic support points. Impulse responses were simulated at the nut, frets, and bridge using vertical, horizontal, and coupling excitation configurations.

C. RESULTS

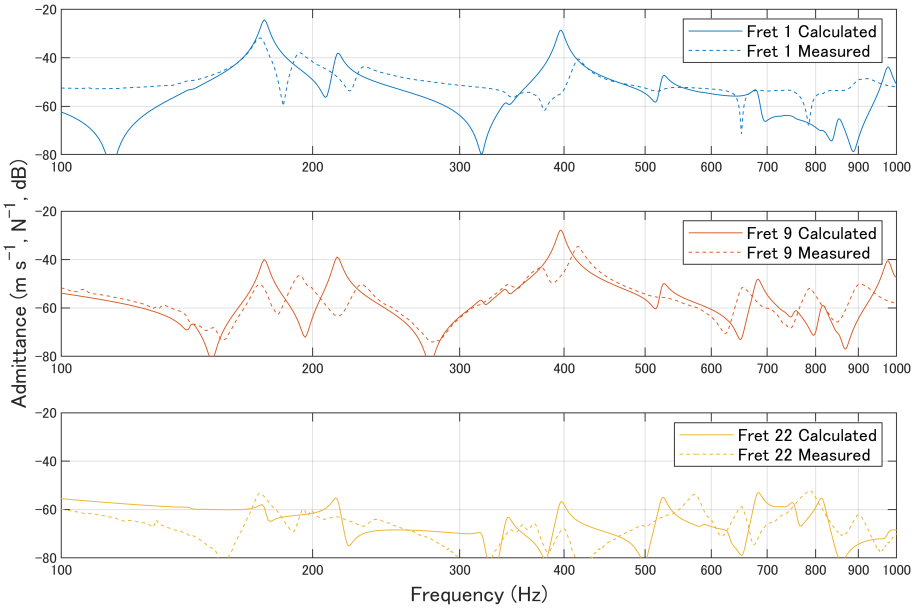

Figure 4: Admittance comparison on vertical measurement

The measured and simulated admittances at frets 1, 13, and 22 under vertical excitation are shown in Fig. 4. While the overall agreement between the measured and simulated results is limited, the discrepancy is likely due to factors such as the presence of a truss rod, string tension, and wood grain orientation—elements that are challenging to incorporate accurately into analytical models. Nevertheless, the trends observed in both measurement and simulation are consistent for typical vibration modes. For instance, at 175 Hz, the amplitude is highest near the headstock at fret 1, while the responses at frets 13 and 22 are significantly lower, demonstrating good agreement between the two approaches.

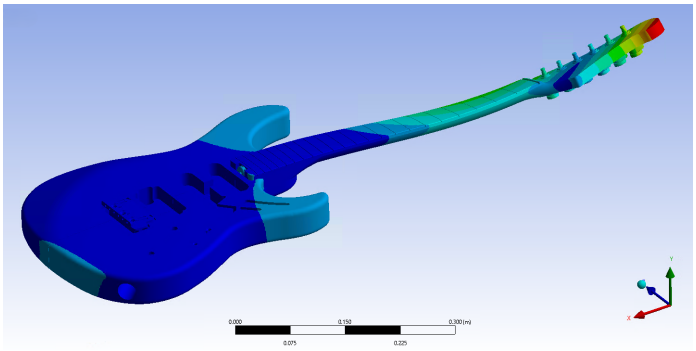

Figure 5: Vibration mode shape of 175Hz on modal analysis

The vibration mode at 175 Hz is illustrated in Fig. 5. In this mode, the body exhibits minimal motion, while the amplitude increases progressively from the middle of the neck (around Fret 9) toward the headstock. The neck undergoes torsional motion and vibrates in both vertical and horizontal directions, resulting in coupling between the two.

The admittance at 175 Hz, as shown in Fig. 3(a) and (b), indicates strong vibration from Fret 9 toward Fret 1 and the nut, consistent with the mode shape observed in Fig. 5. This supports the conclusion that the significant admittance variation—exceeding 40 dB—across frets is primarily caused by the neck's vibrational mode shape.

4. DIGITAL WAVEGUIDE MODELING

A. OBJECTIVES

To incorporate the influence of the guitar body into the DWG model, the vertical, horizontal, and coupling reflection functions of each fret were imported into the model.

B. METHODS

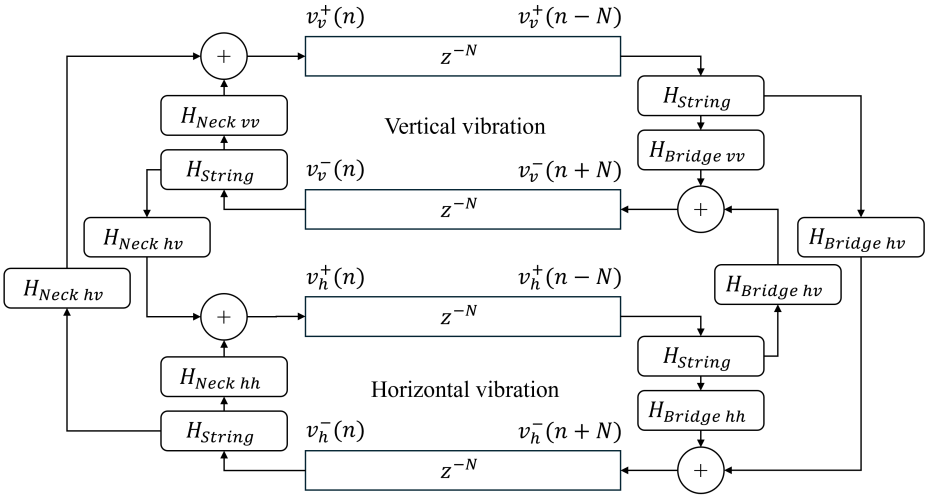

Figure 6: Block diagram of the coupled digital waveguide model of plucked strings

A digital waveguide (DWG) model of the velocity wave of plucked strings, incorporating coupled vertical and horizontal vibrations as illustrated in Fig. 6, was implemented.[4, 9, 10] Reflection functions derived from the measured admittance in Fig. 2(a) and (b) were assigned to the bridge and frets, which serve as reflection boundaries. Additionally, the transfer function obtained from Fig. 2(c) was used to model the coupling between vertical and horizontal vibrations. Damping effects due to air viscosity and internal string losses were implemented at the terminations using a low-pass filter.[11] The physical parameters of the low E string, which was tuned to E2, were determined based on experimental measurements and previously published data.[12]

The initial displacement was set by lifting a segment of the string vertically by 1 mm, while the horizontal displacement was set to 0 mm.

When no fret is pressed, the reflection function of the nut is incorporated into the model. When a fret is pressed, the reflection function corresponding to that specific fret position is applied.

C. RESULTS

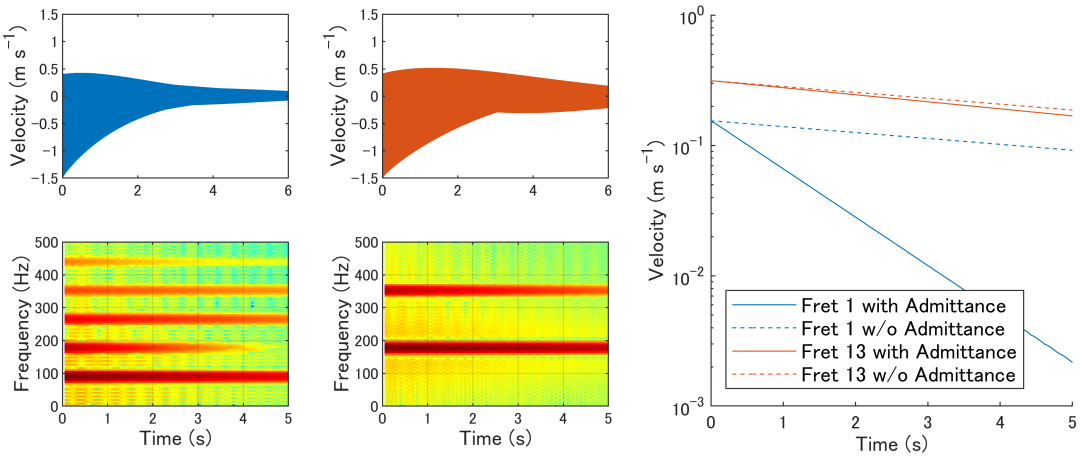

(a) Fret 1 (b) Fret 13 (c) Amplitude transition of 175 Hz

Figure 7: Synthesized vertical velocity waveform and amplitude envelopes for fret 1 and 13 of the low E string.

The vertical velocity waveforms of the string when frets 1 and 13 are pressed are shown in Fig. 7(a) and (b). The 175 Hz component discussed in Fig. 5 appears as a second harmonic at fret 1 and as the fundamental frequency at fret 13. As illustrated in the amplitude transitions in Fig. 7(c), the 175 Hz component decays more rapidly at fret 1. This is attributed to the admittance at fret 1 being 37 dB higher than that at fret 13, as shown in Fig. 2(a).

Notably, when waveform synthesis is performed without incorporating the neck reflection function into the DWG model, the decay rates for both cases are governed solely by string damping and remain nearly identical, as indicated by the dotted line. This modeling approach successfully captures the decay ratio variations observed in the measurements presented in Fig. 2.

5. VERIFICATION OF THE DECAY RATES

A. OBJECTIVES

To verify the accuracy of the fret-dependent decay ratio variations in the DWG model, string vibrations were measured.

B. METHODS

Figure 8: String vibration measurement using wire breaking method

The same guitar used for admittance measurements in Section 2 was employed in this experiment. To prevent frequency shifts in string vibration caused by magnetic attraction, the magnetic pickup was removed.[13] All strings except the vibrating low E string were muted using soft cloth. Frets 1 through 14 were sequentially

pressed using a commercially available capo. A three-axis accelerometer was mounted on the bridge to record acceleration waveforms.

The wire-breaking method was used to excite the strings: a thin 0.063 mm magnet wire was pulled vertically at the same location as the initial displacement defined in the DWG model, and excitation occurred upon the wire's natural breakage.[14]

Acceleration waveforms were recorded four times at each fret position. The logarithmic decay rates of individual harmonic components were calculated and averaged, with outliers excluded.

C. RESULTS

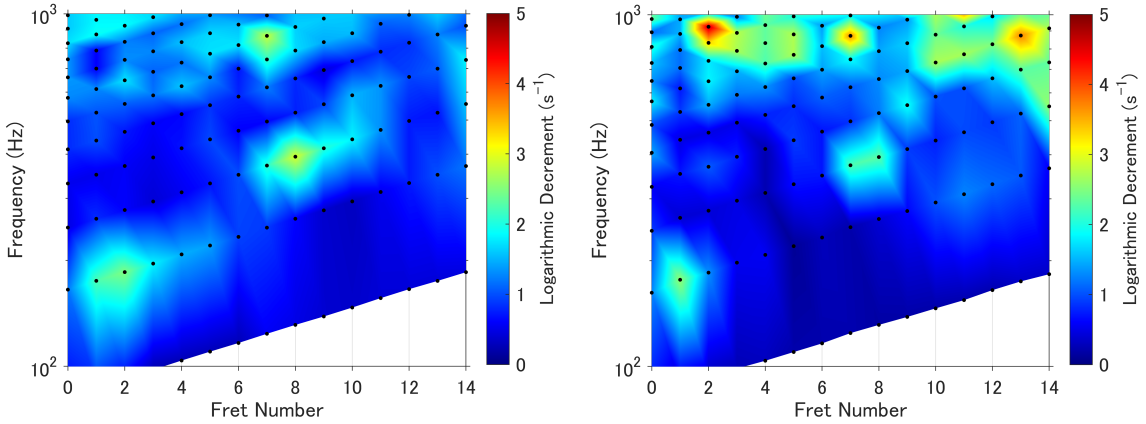

(a) Synthesized by DWG model (b) Measured by accelerometer on bridge

Figure 9: Distribution of the decay rate of each harmonic component in the vibration waveform

Figure 9 presents the logarithmic decrement of both the synthesized waveforms generated by the DWG model and the measured acceleration waveforms. The horizontal axis represents the fret number (with 0 corresponding to the nut), black dots indicate harmonic components, and color shading denotes the logarithmic decrement.

In the synthesized results (Fig. 9(a)), higher decay is observed around 175 Hz for lower frets (1 and 2), around 400 Hz for mid-range frets (7–9), and around 900 Hz for fret 7. These patterns closely align with the admittance trends shown in Fig. 2(a).

Similarly, the measured results (Fig. 9(b)) exhibit decay patterns at the same fret positions, confirming that incorporating fret-specific admittance into the model enables accurate reproduction of decay characteristics associated with the body and neck vibrations of the electric guitar.

However, above 700 Hz, the measured waveforms show faster decay than the synthesized ones. This discrepancy is likely due to the soft contact surface of the capo used in the experiment, which may have introduced elastic damping and acted as a low-pass filter.[15] At the same time, the capo probably introduces less damping than would be the case if human fingers were pressing against the strings or a human hand was holding the neck.

6. CONCLUSION

To account for the influence of the guitar body, admittance measurements were taken at all frets of the electric guitar and incorporated into the DWG model. Given the significant variation in neck admittance across fret positions, it was deemed essential to include individual admittance profiles for each fret. Several peak frequencies observed in the measured neck admittance aligned with the FEA results, enabling analysis of the underlying causes of fret-dependent differences. The decay rate trends of each harmonic component showed strong consistency between the synthesized waveforms generated by the DWG model and the experimentally measured waveforms. Additionally, a uniform increase in decay rate was observed at frequencies above 700 Hz, suggesting the presence of a low-pass filtering effect likely introduced by the elasticity of capos.

The admittance variations caused by the performer's left-hand contact with the neck should be considered in future analyses, as such interactions may influence vibrational behavior. Additionally, the DWG model developed in this study is being explored as an interactive design tool for instrument development.

ACKNOWLEDGMENTS

The authors would like to thank the research team in the “Computational Acoustic Modeling Laboratory (CAML)” and “Yamaha research and development department” for their helpful discussions.

REFERENCES

[1] R. R. Boullosa, “Admittance at the frets of a classical guitar,” J. Catgut Acoust. Soc. Series II. **4**(4), 33-36 (2001).

[2] M. Rau, E. Maestre, J. O. Smith, and G. P. Scavone, “An exploration of guitar neck admittance measurements taken at different string stopping locations,” International Symposium on Musical Acoustics. 73-76 (2017).

[3] M. Rau, J. S. Abel, D. James & J. O. Smith, “Electric-to-acoustic pickup processing for string instruments: An experimental study of the guitar with a hexaphonic pickup,” The Journal of the Acoustical Society of America, **150**(1), 385-397 (2021).

[4] Julius O. Smith III, “Physical Audio Signal Processing”, W3K Publishing (2010).

[5] E. Maestre, G. P. Scavone, and J. O. Smith, “Joint modeling of bridge admittance and body radiativity for efficient synthesis of string instrument sound by digital waveguides,” IEEE/ACM Transactions on Audio, Speech, and Language Processing. **25**(5), 1128-1139 (2017).

[6] B. Bank, and M. Karjalainen, “Passive admittance matrix modeling for guitar synthesis,” In Proc. Conf. on Digital Audio Effects. 3-8 (2010).

[7] E. Maestre, G. P. Scavone, & J. O. Smith, “Digital modeling of bridge driving-point admittances from measurements on violin-family instruments,” In Proc. of the Stockholm Music Acoustics Conference. 101-108 (2013).

[8] E. Maestre, G. P. Scavone, and J. O. Smith, “Digital modeling of string instrument bridge reflectance and body radiativity for sound synthesis by digital waveguides,” In 2015 IEEE Workshop on Applications of Signal Processing to Audio and Acoustics (WASPAA). IEEE. 1-5 (2015).

[9] G. Evangelista, “Physically inspired playable models of guitar, a tutorial. In 2010 4th International Symposium on Communications,” Control and Signal Processing (ISCCSP). IEEE. 1-4 (2010).

[10] M. Rau, and J. O. Smith, “Measurement and modeling of a resonator guitar,” Proceedings of the ISMA. 269-276 (2019).

[11] H. Mansour, J. Woodhouse, and G. P. Scavone. "Enhanced wave-based modelling of musical strings. Part 1: Plucked strings," Acta Acustica united with Acustica. **102**(6), 1082-1093 (2016).

[12] D. R. Grimes, “String theory-the physics of string-bending and other electric guitar techniques,” PloS one. **9**(7), e102088 (2014).

[13] J. Feinberg, and B. Yang, “Natural-frequency splitting of a guitar string caused by a non-uniform magnetic field,” The Journal of the Acoustical Society of America, **144**(5), EL460-EL464 (2018).

[14] G. O. Paiva, F.Ablitzer, F. Gautier, and J. M. C. dos Santos, “The Roving Wire-Breaking Technique: a low cost mobility measurement procedure for string musical instruments,” Applied Acoustics, **139**, 140-148 (2018).

[15] G Evangelista & F. Eckerholm, “Player–instrument interaction models for digital waveguide synthesis of guitar: Touch and collisions,” IEEE transactions on audio, speech, and language processing, **18**(4), 822-832 (2010).

[16] V. Fréoura, H. Mansoura, C. Saitisa, and G. P. Scavone, “Evaluation and classification of steel string guitars using bridge admittances,” IsmAΓ14. Le mans. France. (2014).

[17] J. Woodhouse, D. Politzer, and H. Mansour, “Acoustics of the banjo: measurements and sound synthesis,” Acta Acustica **5**, 15 (2021).